Letters

A Simultaneous Power and Data Transmission Technology Based on Coil Multiplexing in Domino-Resonator WPT Systems

Yong Li, *Senior Member, IEEE*, Xiao Yang, Wenjun Sun, Jiefeng Hu, and Zhengyou He, *Senior Member, IEEE*

***Abstract*—To achieve parallel power and data transmission in domino-resonator wireless power transfer (WPT) systems, a novel simultaneous power, and data transfer (SPDT) technology based on coil multiplexing is proposed in this letter. Benefiting from the magnetic field characteristics of the bipolar coil structure, the power and data can be injected into multiplexed coils with different flow directions, leading to opposite induced voltage polarities in each coupling coil. Subsequently, a corresponding resonator circuit is developed to form independent power and data resonance loops. In addition, an injected data transmission scheme is developed for domino-resonator WPT systems. Compared with traditional SPDT methods, additional wave trappers and coupling structures are avoided by this proposed technology, and the interference between power and data transfer is significantly eliminated. A 23.6 W laboratory prototype with five domino resonators is built to validate the feasibility of this proposed technology. The experimental results show that the power transfer efficiency reaches 70% at 50 kb/s data transfer rate.**

***Index Terms*—Coil multiplexing, domino-resonator, simultaneous power and data transfer (SPDT), wireless power transfer (WPT).**

I. Introduction

ONLINE health monitoring equipment has been widely deployed in high voltage (HV) electrical networks to detect system operation performance, serving as the cornerstone of modern smart grid construction [1]. Such monitoring equipment needs to function autonomously in a 24/7 manner. In this context, the stable power supply and reliable data transfer methods have, therefore, become highly crucial for online monitoring system development. Traditional self-powered technologies use solar or wind as the power source for grid monitoring applications. However, this kind of power source is subject to varied weather conditions and geographical locations. Nowadays, current transformers can harvest the continuous magnetic energy from power lines on the high voltage side, which can provide a weather-independent and stable power supply. To power the monitoring equipment on the low-voltage transmission tower, a safe and efficient power transfer technology over a long creepage distance should be studied [2]. In comparison to transformers, the domino-resonator wireless power transfer (WPT) technology shows outstanding insulation properties [2], [3], [4], [5], therefore, the harvested power can be transmitted wirelessly over the insulation distance from the HV side to the ground. Furthermore, all the domino-resonator coils can be embedded in insulator without requiring additional volume, which has no influence on the function of the insulator [5], [6]. A typical five-domino-resonator WPT system structure for a 35-kV insulator is shown in Fig. 1.

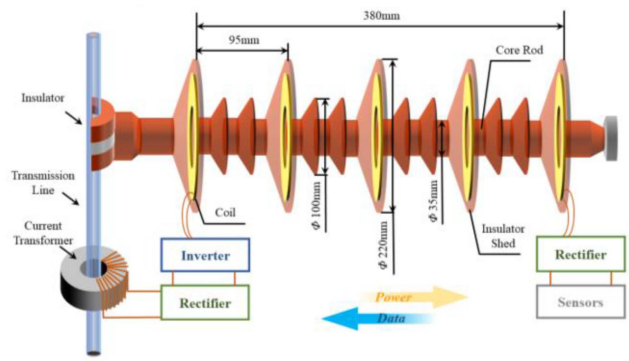

Fig. 1. Structure diagram of five-domino-resonator WPT system embedded in 35 kV insulator.

In addition to the power requirement, the reliable communication between transmitters and receivers is also essential for domino-resonator WPT systems, especially in real-time output power regulation and monitoring information feedback. Thanks to the advantages of limited system cost, low transmission delay and strong immunity to interference, the simultaneous power,

Manuscript received 31 August 2022; revised 1 October 2022 and 10 November 2022; accepted 24 November 2022. Date of publication 29 November 2022; date of current version 26 December 2022. This work was supported in part by Young Elite Scientist Sponsorship Program by China Association for Science and Technology, in part by the Star of Science and Technology in Southwest Jiaotong University under Grant 2682021CG018, in part by Young Eagle Program in Southwest Jiaotong University, and in part by Young Crops Program in Southwest Jiaotong University. *(Corresponding author: Yong Li.)*

Yong Li, Xiao Yang, Wenjun Sun, and Zhengyou He are with the School of Electrical Engineering, Southwest Jiaotong University, Chengdu 610031, China (e-mail: leeo1864@163.com; yangxiao@my.swjtu.edu.cn; wenjss@163.com; hezy@swjtu.edu.cn).

Jiefeng Hu is with the Institute of Innovation, Science, and Sustainability, Federation University Australia, Mount Helen, VIC 3353, Australia, and also with the Centre for New Energy Transition Research, Federation University Australia, Mount Helen, VIC 3353, Australia (e-mail: j.hu@federation.edu.au).

Color versions of one or more figures in this article are available at https://doi.org/10.1109/TPEL.2022.3225479.

Digital Object Identifier 10.1109/TPEL.2022.3225479

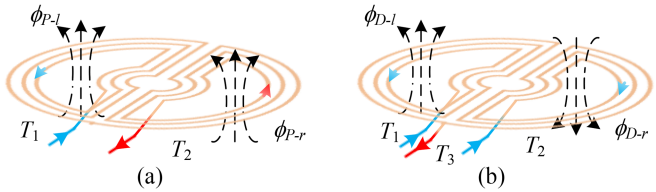

Fig. 2. Coil multiplexing method with different magnetic polarity generated by (a) power and (b) data.

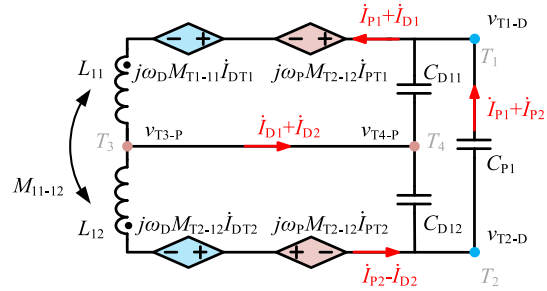

Fig. 3. Compensation circuit for power and data.

and data transmission (SPDT) technology has substantial application value in WPT systems [7]. After decades of development, the research of SPDT technology can now be categorized into three research areas: 1) additional coupling, 2) power modulation, and 3) data injection.

As to the additional coupling methods, supplementary coils or metal plates are usually utilized to build the data transfer channel [8]. Considering the numerous relays in domino-resonator WPT systems, a large number of components should be used to ensure the coupling in data transmission, which leads to a huge increase in system volume and cost. Additionally, there is non-negligible interference between power and data transmission channels, which can spoil the received data quality [8]. As regards the power modulation methods, data are transmitted through the discrete operation mood shift of the inverter or additional switch [10]. The data transmission rate is greatly limited by the power transfer frequency, and the modulation of power inevitably deteriorates the system efficiency and the output power stability [11]. The third research area, i.e., data injection methods, aims to achieve SPDT with a high data transmission rate, where data and power share the same coupling mechanism [12]. In traditional data injection schemes, the crosstalk between power and data is mitigated by harsh wave trappers on both transmitter and receiver sides [13]. However, due to the lack of data resonance loop, the data cannot pass through the intermediate resonators in domino-resonator WPT systems, and the introduction of filter components significantly augments system cost and circuit complexity.

In this letter, a novel simultaneous power and data transmission technology based on coil multiplexing is proposed. Benefiting from the magnetic field characteristics of bipolar coil, the power and data own its specific resonance loop in each resonator. Specifically, the power and data are injected, respectively, into multiplexed bipolar coils from different terminals, and the current blocks for power and data can be founded at different compensation components. Thus, the independent power and data transmission channels can be built simultaneously in the same coupling mechanisms. Without the need for additional coupling structures or embedded wave trappers, the interference between power and data transmission is naturally reduced.

II. Resonator Circuit Design

The magnetic field characteristics of a bipolar coil structure is illustrated in Fig. 2, in which the power and data are injected into the multiplexed coil from different coil terminals. In this case, power flow follows the path from T_1 to T_2, while data is injected from T_1 and T_2 at the same time, and extracted from the midpoint T_3 of two single polar coils. According to Ampere's law, the magnetic polarity is in accordance with the current flow direction. In this letter, the power current flows in a counterclockwise direction in both left and right semicircles, while data currents flow counterclockwise in the left semicircle and clockwise in the right semicircle. Thus, the magnetic fluxes generated by power current $\phi_{P\text{-}l}$ and $\phi_{P\text{-}r}$ in Fig. 2(a) have the same propagation direction, whereas the magnetic fluxes generated by data current $\phi_{D\text{-}l}$ and $\phi_{D\text{-}r}$ in Fig. 2(b) show the opposite result.

The propagation direction of magnetic flux is represented in the circuit as the polarity of induced voltage. To accommodate different induced voltage polarities, a specific compensation circuit is developed to form independent data and power resonance loops. The first intermediate resonator in domino-resonator SPTD system is taken, as an example in Fig. 3, where L_{11} and L_{12} are the single polar coil parts from one complete bipolar coil, and $M_{11\text{-}12}$ is the non-negligible mutual inductance between L_{11} and L_{12}. $C_{\mathrm{D}11}$, $C_{\mathrm{D}12}$, and $C_{\mathrm{P}1}$ are used to compensate the data and power circuits for achieving resonance state, respectively.

The power and data induced voltages are simultaneously generated in the bipolar coil, where $M_{\mathrm{T1\text{-}11}}$ and $M_{\mathrm{T2\text{-}12}}$ are the mutual inductances between the transmitter coil and the premier intermediate coil. Additionally, ω_{P} and ω_{D} represent the power and data angular frequency, and $\dot{I}_{\mathrm{DT1(2)}}$ and $\dot{I}_{\mathrm{PT1(2)}}$ are the power and data current in the transmitter polar coil, respectively. Each polar coil should be wound with the same parameters, therefore, we have

$$L_{11} = L_{12}, C_{\mathrm{D}11} = C_{\mathrm{D}12}, M_{\mathrm{T1-11}} = M_{\mathrm{T2-12}}. \tag{1}$$

Accordingly, the power and data current in each polar coil should be equal.

$$\begin{cases} \dot{I}_{\mathrm{DT1}} = \dot{I}_{\mathrm{DT2}} \\ \dot{I}_{\mathrm{PT1}} = \dot{I}_{\mathrm{PT2}}. \end{cases} \tag{2}$$

As shown in Fig. 3, the power and data induced voltages share the same polarity in L_1, while the opposite polarity in L_2. Herein, on the one hand, the power voltage at terminal T_3 and terminal T_4 should be equal, i.e., $v_{\mathrm{T3\text{-}P}} = v_{\mathrm{T4\text{-}P}}$, and the current flows through T_3 and T_4 only has the data current $\dot{I}_{\mathrm{D1}} + \dot{I}_{\mathrm{D2}}$; on the other hand, the data voltage at terminal T_1 and point T_2 should be equal, i.e., $v_{\mathrm{T1\text{-}D}} = v_{\mathrm{T2\text{-}D}}$, and the current flows through T_1 and point T_2 only has the power current $\dot{I}_{\mathrm{P1}} + \dot{I}_{\mathrm{P2}}$. Therefore, the

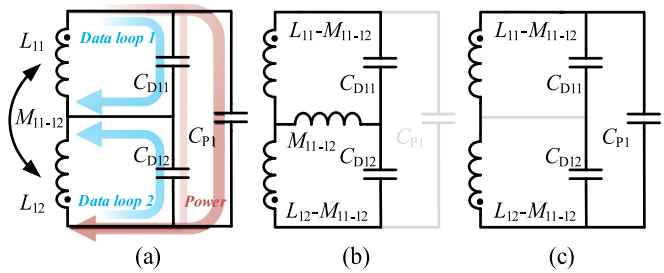

Fig. 4. Illustration of (a) power and data independent resonance loops, (b) equivalent data resonance circuit, and (c) equivalent power resonance circuit.

interference between power and data can be naturally eliminated by the proposed compensation circuit.

The independent power and data resonance loops in the first resonator are shown in Fig. 4(a). It could be found that little power current passes C_{D11} and C_{D12}, which does not affect the independence between power and data in specific resonance loops. Considering the mutual inductance $M_{11\text{-}12}$ between L_{11} and L_{12}, the equivalent data resonance circuit can be found in Fig. 4(b). Since the inductance and capacitance values in each data loop are identical, the data current in each loop should also be the same. The data resonance frequency f_{DR} is further determined by

$$f_{\mathrm{DR}} = \frac{1}{2\pi\sqrt{(L_{11}+M_{11\text{–}12})C_{\mathrm{D11}}}} = \frac{1}{2\pi\sqrt{(L_{12}+M_{11\text{–}12})C_{\mathrm{D12}}}}. \tag{3}$$

Similarly, the equivalent power resonance circuit can also be established in Fig. 4(c). Given that the data transfer frequency is at least one order of magnitude larger than the power transfer frequency, the power resonance frequency f_{PR} is expressed as

$$f_{\mathrm{PR}} = \frac{1}{2\pi\sqrt{(L_{11}+L_{12}-2M_{11\text{–}12})(\frac{C_{\mathrm{D11}}+C_{\mathrm{D12}}}{C_{\mathrm{D11}}C_{\mathrm{D12}}}+C_{\mathrm{P1}})}} \approx \frac{1}{2\pi\sqrt{(L_{11}+L_{12}-2M_{11\text{–}12})C_{\mathrm{P1}}}}. \tag{4}$$

III. Proposed Domino-Resonator System

A. Structure of SPDT System

The architecture of the proposed five-domino-resonator SPDT system is illustrated in Fig. 5, where each resonator has the same compensation topology design. In this demonstration of backward data transfer, the data are injected from the power receiver side and extracted from the power transmitter side, via high-frequency coupled transformers. Moreover, the ON–OFF keying data modulation is applied here to test the feasibility of the data transfer. In this letter, the power and data resonance frequencies are set to 200 kHz and 1 MHz, respectively.

In Fig. 5, U_{dc} is the input dc voltage source connected to the rectifier on the transmitter side, and U_{L} is the output voltage of the load resistance R_{L}. S_1–S_4 and D_1–D_4 constitute the inverter and rectifier. L_{Ti}, L_{ji}, and L_{Ri} (i = 1, 2, j = 1, 2, 3) constitute the multiplexed transmitter, intermediate, and receiver coils, respectively, and r_{Ti}, r_{ji}, and r_{Ri} (i = 1, 2, j = 1, 2, 3)

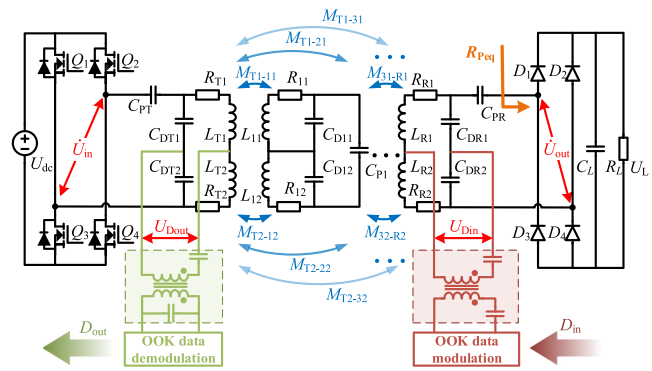

Fig. 5. Architecture of domino-resonator SPDT system.

TABLE I
Simulated Coil Inductance

Parameter	Value	Parameter	Value
L_{T1}	98.97 μH	$M_{\mathrm{T1\text{-}11}}$	5.29 μH
L_{T2}	98.84 μH	$M_{\mathrm{T1\text{-}21}}$	1.12 μH
$M_{\mathrm{T1\text{-}T2}}$	7.71 μH	$M_{\mathrm{T1\text{-}31}}$	0.38 μH
$M_{\mathrm{T1\text{-}12}}$	0.90 μH	$M_{\mathrm{T1\text{-}R1}}$	0.17 μH

are parasitic resistances of coils. The compensation capacitor C_{PT}, C_{DTi}, C_{Pj}, C_{Dji}, C_{PR}, and C_{DRi} (i = 1, 2, j = 1, 2, 3) are integrated into each resonator to form independent power and data resonance loops. The $M_{\mathrm{xi\text{-}yj}}$ (x, y = T, 1, 2, 3, R; i, j = 1, 2) is the mutual inductance between polar coil L_{xi} and L_{yi}. To simplify the whole SPDT system analysis, the transmitting coil, the receiving coil, and the intermediate coils own the same dimensions and number of turns in this letter. Consequently, the self-inductance, the compensating capacitance, and the mutual inductance between adjacent coils are set at the same value.

Through finite element model simulation, the inductance with the transmitter coil can be obtained in Table I. The mutual inductances with other intermediate coils and receiver coil follow the same law as the transmitter coil. It should be emphasized that the mutual inductance between non-aligned polar coils, e.g., $M_{\mathrm{T1\text{-}12}}$, is relatively small. Thus, its influence on the power and data transmission is limited.

B. Analysis of Power Transmission Channel

The fundamental component approximation method is applied here to analyze the power transmission channel. The inverter output voltage in phasor form follows $\dot{U}_{\mathrm{in}} = 2\sqrt{2}/\pi \cdot U_{\mathrm{dc}}$. R_{Peq} is the equivalent input resistance of the rectifier, which satisfies $R_{\mathrm{eq}} = 8/\pi^2 \cdot R_{\mathrm{L}}$. The impedance of each resonator in power loop Z_{Pi} (i = T, 1, 2, 3, R) is defined as

$$Z_{\mathrm{Pi}} = j\omega_{\mathrm{P}}L_{\mathrm{i1}} + j\omega_{\mathrm{P}}L_{\mathrm{i2}} - 2j\omega_{\mathrm{P}}M_{\mathrm{i1\text{–}i2}} + \frac{1}{j\omega_{\mathrm{P}}C_{\mathrm{Pi}}} + r_{\mathrm{i1}} + r_{\mathrm{i2}}. \tag{5}$$

Due to the same power current direction in both left and right semicircles, the mutual inductance between nonaligned polar coils will strengthen power transmission channel coupling. $M_{\mathrm{P:x\text{-}y}}$ (x, y = T, 1, 2, 3, R) is defined as the equivalent power mutual inductance between bipolar coils, which is given by $M_{\mathrm{P:x\text{-}y}} = M_{\mathrm{x1\text{-}y1}} + M_{\mathrm{x2\text{-}y2}} + M_{\mathrm{x1\text{-}y2}} + M_{\mathrm{x2\text{-}y1}}$.

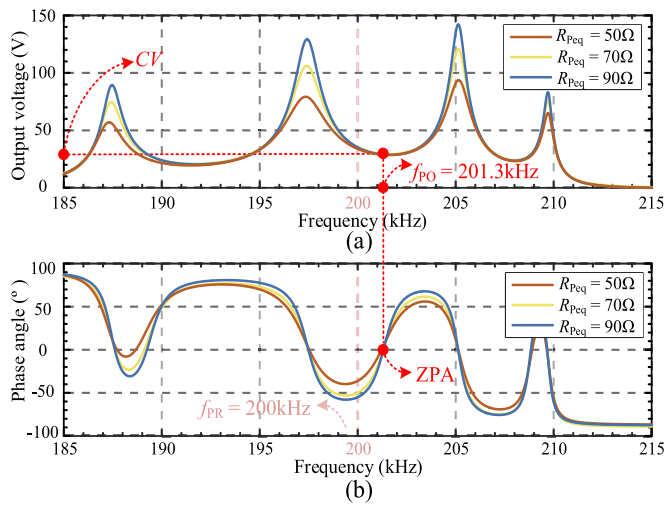

Fig. 6. CV output characteristics of domino-resonator WPT system. (a) Output voltage U_{out}. (b) Phase angle.

Applying Kirchhoff's voltage law (KVL), the power transmission channel is then derived

$$\begin{bmatrix} Z_{\mathrm{PT}} & -j\omega_{\mathrm{P}}M_{\mathrm{P:T-1}} & \cdots & -j\omega_{\mathrm{P}}M_{\mathrm{P:T-R}} \\ -j\omega_{\mathrm{P}}M_{\mathrm{P:T-1}} & Z_{\mathrm{P1}} & \cdots & -j\omega_{\mathrm{P}}M_{\mathrm{P:1-R}} \\ \vdots & \vdots & \ddots & \vdots \\ -j\omega_{\mathrm{P}}M_{\mathrm{P:T-R}} & -j\omega_{\mathrm{P}}M_{\mathrm{P:1-R}} & \cdots & Z_{\mathrm{PR}}+R_{\mathrm{Peq}} \end{bmatrix} \cdot \begin{bmatrix} \dot{I}_{\mathrm{PT}} \\ \dot{I}_{\mathrm{P1}} \\ \vdots \\ \dot{I}_{\mathrm{PR}} \end{bmatrix} = \begin{bmatrix} \dot{U}_{\mathrm{in}} \\ 0 \\ \vdots \\ 0 \end{bmatrix} \tag{6}$$

where $\dot{I}_{\mathrm{Pi}}$ (i = T, 1, 2, 3, R) are the phasors of power current in each resonator. The system output voltage U_{out} can further be expressed as

$$U_{\mathrm{out}} = i_{\mathrm{PR}} \cdot R_{\mathrm{Peq}}. \tag{7}$$

Moreover, the power voltage gain is obtained as

$$G_{\mathrm{P}} = \left|\frac{U_{\mathrm{out}}}{U_{\mathrm{in}}}\right| = \left|\frac{i_{\mathrm{PR}}R_{\mathrm{Peq}}}{U_{\mathrm{Pin}}}\right|. \tag{8}$$

Regarding the unique multicoil structure, the key factor affecting the domino-resonator system efficiency is the current in each resonator. The system transfer efficiency, calculated from the ratio between load output power and the transmitter coil input power, is expressed as

$$\eta = \frac{i_{\mathrm{PR}}^2 \cdot R_{\mathrm{Peq}}}{i_{\mathrm{PR}}^2 \cdot R_{\mathrm{Peq}} + i_{\mathrm{PR}}^2 \cdot (r_{\mathrm{R1}}+r_{\mathrm{R2}}) + i_{\mathrm{T}}^2 \cdot (r_{\mathrm{T1}}+r_{\mathrm{T2}}) + \sum_{\mathrm{i}=1}^{3} i_{\mathrm{Pi}}^2 \cdot (r_{\mathrm{i1}}+r_{\mathrm{i2}})}. \tag{9}$$

According to the KVL expression of the power transmission channel in (6), high-order simultaneous equations need to be solved to get U_{out}. The computer analysis is further used here to visualize the system voltage output U_{out} and system input phase angle, as plotted in Fig. 6. Due to cross-coupling between nonadjacent coils, the system operation frequency f_{PO} should shift slightly from the designed power resonance frequency f_{PR} [5]. Therefore, the domino-resonator WPT system is still able to achieve both zero phase align and constant voltage (CV) output characteristics at 201.3 kHz.

C. Analysis of Data Transmission Channel

Since the parameter of data loop in each resonator is identical, the data current in each loop should also be the same. $\dot{I}_{\mathrm{Di}}$ (i = T, 1, 2, 3, R) is defined as the phasors of data current

$$\dot{I}_{\mathrm{Di}} = \dot{I}_{\mathrm{Di1}} = \dot{I}_{\mathrm{Di2}}. \tag{10}$$

Similarly, the impedance of each resonator in data loop Z_{Di} (i = T, 1, 2, 3, R) can also be represented as

$$Z_{\mathrm{Di}} = Z_{\mathrm{Di1}} = Z_{\mathrm{Di2}} = j\omega_D L_{\mathrm{i1}} + j\omega_D M_{\mathrm{i1\text{–}i2}} + \frac{1}{j\omega_D C_{\mathrm{Di1}}} + r_{\mathrm{i1}}. \tag{11}$$

Due to the opposite current direction between two data loops, the mutual inductance between nonaligned polar coils, will slightly weaken the data transmission channel coupling. $M_{\mathrm{D:x\text{-}y}}$ (x, y = T, 1, 2, 3, R) is defined as the equivalent data mutual inductance between polar coils, which is defined as $M_{\mathrm{D:x\text{-}y}} = M_{\mathrm{D1:x\text{-}y}} = M_{\mathrm{D2:x\text{-}y}} = M_{\mathrm{x1\text{-}y1}} - M_{\mathrm{x2\text{-}y1}} = M_{\mathrm{x2\text{-}y2}} - M_{\mathrm{x1\text{-}y2}}$.

The first data transmission channel of the domino-resonator SPDT system is given by KVL

$$\begin{bmatrix} Z_{\mathrm{DT1}} & -j\omega_{\mathrm{D}}M_{\mathrm{D1:T-1}} & \cdots & -j\omega_{\mathrm{D}}M_{\mathrm{D1:T-R}} \\ -j\omega_{\mathrm{D}}M_{\mathrm{D1:T-1}} & Z_{\mathrm{D11}} & \cdots & -j\omega_{\mathrm{P}}M_{\mathrm{D1:1-R}} \\ \vdots & \vdots & \ddots & \vdots \\ -j\omega_{\mathrm{D}}M_{\mathrm{D1:T-R}} & -j\omega_{\mathrm{D}}M_{\mathrm{D1:1-R}} & \cdots & Z_{\mathrm{DR1}}+2R_{\mathrm{Deq}} \end{bmatrix} \cdot \begin{bmatrix} \dot{I}_{\mathrm{DT1}} \\ \dot{I}_{\mathrm{D11}} \\ \vdots \\ \dot{I}_{\mathrm{DR1}} \end{bmatrix} = \begin{bmatrix} \dot{U}_{\mathrm{Din}} \\ 0 \\ \vdots \\ 0 \end{bmatrix}. \tag{12}$$

The second data transmission channel of the domino-resonator SPDT system is given by KVL

$$\begin{bmatrix} Z_{\mathrm{DT2}} & -j\omega_{\mathrm{D}}M_{\mathrm{D2:T-1}} & \cdots & -j\omega_{\mathrm{D}}M_{\mathrm{D2:T-R}} \\ -j\omega_{\mathrm{D}}M_{\mathrm{D2:T-1}} & Z_{\mathrm{D12}} & \cdots & -j\omega_{\mathrm{P}}M_{\mathrm{D2:1-R}} \\ \vdots & \vdots & \ddots & \vdots \\ -j\omega_{\mathrm{D}}M_{\mathrm{D2:T-R}} & -j\omega_{\mathrm{D}}M_{\mathrm{D2:1-R}} & \cdots & Z_{\mathrm{DR2}}+2R_{\mathrm{Deq}} \end{bmatrix} \cdot \begin{bmatrix} \dot{I}_{\mathrm{DT2}} \\ \dot{I}_{\mathrm{D12}} \\ \vdots \\ \dot{I}_{\mathrm{DR2}} \end{bmatrix} = \begin{bmatrix} \dot{U}_{\mathrm{Din}} \\ 0 \\ \vdots \\ 0 \end{bmatrix}. \tag{13}$$

In (12) and (13), R_{Deq} is the equivalent input resistance of the data demodulation circuit, and the load current is composed of two loops together. Consequently, the data voltage gain is

$$G_{\mathrm{D}} = \left|\frac{U_{\mathrm{Dout}}}{U_{\mathrm{Din}}}\right| = \left|\frac{(i_{\mathrm{DR1}}+i_{\mathrm{DR2}})R_{\mathrm{Deq}}}{U_{\mathrm{Din}}}\right| = \left|\frac{2i_{\mathrm{DR}}R_{\mathrm{Deq}}}{U_{\mathrm{Din}}}\right|. \tag{14}$$

For data transfer channel, the dynamic response can be treated as a zero-state response approximately, and the duration of the transient process is the main limit of the communication data

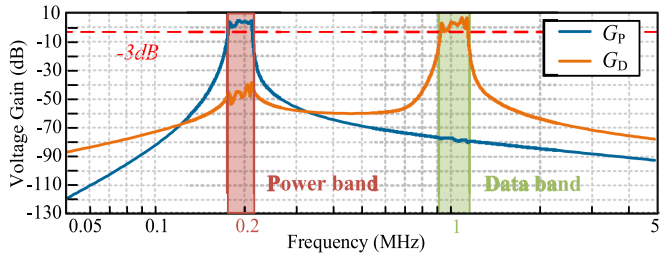

Fig. 7. Frequency response of domino-resonator WPT system.

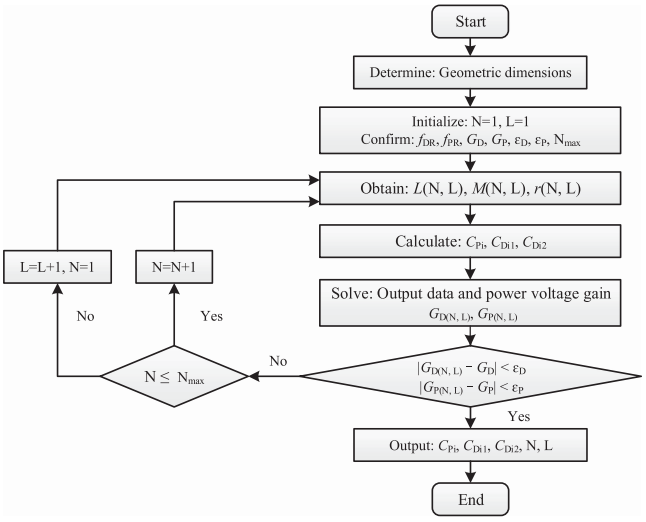

Fig. 8. SPDT system design process diagram.

rate. According to [14], when the induced voltage reaches 95%, the output could be viewed to be stable, and the transient time of data resonator i can be calculated by

$$t_{di} = \frac{6(L_{i1} + \sum M_{i1-j1})}{r_{i1} + \sum R_{ref(i1-j1)}} = \frac{6(L_{i2} + \sum M_{i2-j2})}{r_{i2} + \sum R_{ref(i2-j2)}} \quad (15)$$

where $R_{ref(i1-j1)}$ and $R_{ref(i2-j2)}$ are the first and second reflected impedance of resonator j to i (i, j = T, 1, 2, 3, R, j ≠ i), respectively. In theory, the maximum transfer rate is dependent on the maximum response time, and the data rate can be obviously improved by the increment of the loop impedance. However, the data loss and the demodulation ability (low-noise and high-accuracy signal demodulation) should be synthetically considered to choose the series resistance value [15].

Considering the mutual inductance between non-adjacent coils, the power and data voltage gain are plotted in Fig. 7. Both G_P and G_D can achieve high values in their expected frequency band, while the output gain in each other's band is always less than −40 db. Thus, the crosstalk between power and data is significantly reduced, which results in independent transfer channels and guarantees accurate data demodulation.

D. SPDT System Design Process

To further elaborate the SPDT system design process, a diagram is presented in Fig. 8. The geometric dimensions of the domino-resonator system, e.g., coil size, number, and the air gap, should be first determined according to the insulator model. Subsequently, the initial coil turns N and layers L are both set as one, and the data and power resonance frequency (f_{DR}, f_{PR}), voltage gain (G_D, G_P), error coefficient (ε_D, ε_P), and maximum coil turns in each layer should be confirmed. L(N, L), M(N, L), R(N, L) are the matrix of self-inductance, mutual inductance, and resistance, which can be obtained by simulation or experiment. After the calculation of C_{Pi}, C_{Di1}, C_{Di2}, the power and data output gain G_P(N, L), and G_D(N, L) can be solved at proper operation frequency band. The design process will go into the iteration statement if $|G_D(N, L)–G_D| > \varepsilon_D$ and $|G_P(N, L)–G_P| > \varepsilon_P$. Otherwise, C_{Pi}, C_{Di1}, C_{Di2}, N, and L serve as the output of the design process.

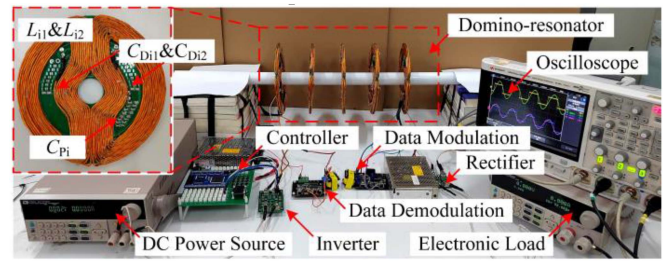

Fig. 9. Experimental prototype.

TABLE II
EXPERIMENTAL SYSTEM PARAMETERS

U_{dc}	f_{PR}	f_{DR}	L_{T1} / L_{T2}	C_{DT1} / C_{DT2}	C_{PT}
35 V	200 kHz	1 MHz	86.2 μH	260 pF	3.8 nF
M_{T1-T2}	M_{T1-12}	M_{T1-11}	M_{T1-21}	M_{T1-31}	M_{T1-R1}
5.4 μH	0.5 μH	4.7 μH	0.8 μH	~ 0 μH	~ 0 μH

IV. EXPERIMENTAL VERIFICATION

To verify the proposed SPDT technology, an experimental prototype of a five-domino-resonator system is set up in Fig. 9. To accommodate the commercial insulator model standard (FXBW-35/70-650) in Fig. 1, the bipolar coil is wound on the 200 mm outer diameter printed circuit board with embedded resonant capacitors. All the polar coils are semicircles with two layers, which have 12 turns litz-wire in each layer. The measured system parameters are listed in Table II, the parameters of each resonator are approximatively identical. It is worth mentioning that, in accordance with the analysis in Section III-B, the power transfer operation frequency f_{PO} is set at 202 kHz, which shifts slightly from f_{PR} due to the cross-coupling between nonadjacent coils.

The measured waveforms in Fig. 10 demonstrate the effectiveness of this proposed SPDT technology under various data rates. A 30 Ω resistance is connected in series to the independent data branch to alleviate the transient time of data transmission, leading to a higher data rate. When the electronic load is receiving power from the dc power source, a continuous data sequence "0101" is injected from the power receiver side, and can be successfully recovered on the power transmitter side,

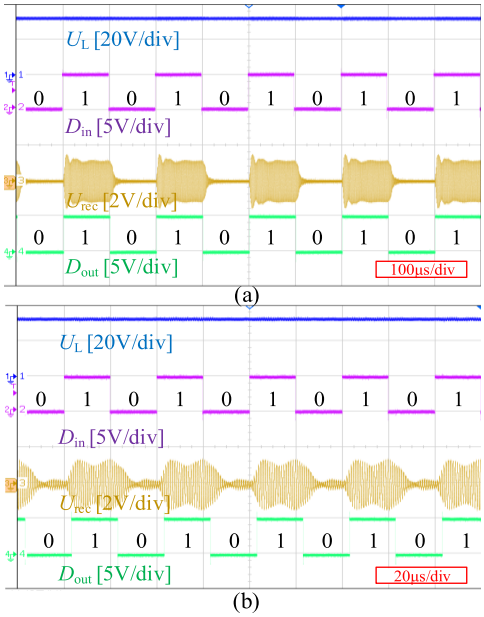

Fig. 10. SPDT measured waveforms with different data rates. (a) In total, 10 kb/s data rate. (b) In total, 50 kb/s data rate.

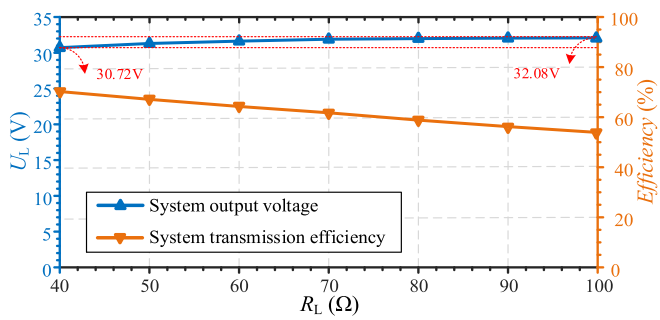

Fig. 11. Measured system output voltage and efficiency against the load.

with 10 kb/s and 50 kb/s data rates, respectively. Also, it can be seen that the limited crosstalk from power does not affect the quality of the received signal U_{rec}. A slight data transmission delay of around 4.2 μs is observed, which is mainly caused by 1) the demodulation circuit and 2) the transient response of data transmission channel. The delay produced by SPDT technology is extremely low, compared to the millisecond delay in conventional wireless communication methods, e.g., Wi-Fi and Bluetooth [7].

Simultaneous power and data transmission capacity should not be achieved by sacrificing the system output performance and efficiency of the WPT system. To validate the effectiveness of the proposed SPDT technology, the system output voltage and transmission efficiency under varying load conditions are measured, as shown in Fig. 11. The maximum system transmission efficiency reaches 70.1% when R_L is equal to 40 Ω. Additionally, it can also be seen that the system output voltage tracks reference tightly, whose variation is less than 5%. This means the proposed system has CV output characteristics.

V. Conclusion

Benefiting from the magnetic field characteristics of bipolar coil, this letter introduces a novel simultaneous power and data transmission technology for domino-resonator WPT systems. All the coupling coils are multiplexed with injected power and data, and two independent flow loops can be formed within the specific compensation circuit. The data transmission has high output gain at data resonance frequency band, and the interference between power and data is significantly reduced. The experimental results prove that the proposed SPDT method can ensure 70% power transmission efficiency, while achieving 50 kb/s data transmission.

References

[1] C. Zhang, D. Lin, N. Tang, and S. Y. R. Hui, "A novel electric insulation string structure with high-voltage insulation and wireless power transfer capabilities," *IEEE Trans. Power Electron.*, vol. 33, no. 1, pp. 87–96, Jan. 2018.

[2] J. Qu and C. K. Lee, "Dynamic modeling for the wireless power transfer system in domino structure," *IEEE Trans. Ind. Electron.*, vol. 69, no. 4, pp. 3556–3565, Apr. 2022.

[3] Y. Li, W. Sun, X. Zhu, and J. Hu, "A hybrid modulation control for wireless power transfer systems to improve efficiency under light-load conditions," *IEEE Trans. Ind. Electron.*, vol. 69, no. 7, pp. 6870–6880, Jul. 2022.

[4] Y. Li et al., "Extension of ZVS region of series–series WPT systems by an auxiliary variable inductor for improving efficiency," *IEEE Trans. Power Electron.*, vol. 36, no. 7, pp. 7513–7525, Jul. 2021.

[5] Z. Yan et al., "A monitoring equipment charging system for HVTL based on domino-resonator WPT with constant current or constant voltage output," *IEEE Trans. Power Electron.*, vol. 37, no. 3, pp. 3668–3680, Mar. 2022.

[6] Z. Dong, S. Liu, X. Li, Z. Xu, and L. Yang, "A novel long-distance wireless power transfer system with constant current output based on domino-resonator," *IEEE J. Emerg. Sel. Topics Power Electron.*, vol. 9, no. 2, pp. 2343–2355, Apr. 2021.

[7] Y. Yao, P. Sun, X. Liu, Y. Wang, and D. Xu, "Simultaneous wireless power and data transfer: A comprehensive review," *IEEE Trans. Power Electron.*, vol. 37, no. 3, pp. 3650–3667, Mar. 2022.

[8] X. Li et al., "An inductive and capacitive combined parallel transmission of power and data for wireless power transfer systems," *IEEE Trans. Power Electron.*, vol. 33, no. 6, pp. 4980–4991, Jun. 2018.

[9] G. Wang, P. Wang, Y. Tang, and W. Liu, "Analysis of dual band power and data telemetry for biomedical implants," *IEEE Trans. Biomed. Circuits Syst.*, vol. 6, no. 3, pp. 208–215, Jun. 2012.

[10] H. Li, S. Chen, J. Fang, and K. Wang, "Frequency-modulated phase shift keying communication for MEPT control of wireless power transfer," *IEEE Trans. Power Electron.*, vol. 36, no. 5, pp. 4954–4959, May 2021.

[11] X. Liu, C. Xia, X. Han, Z. Wu, and Z. Liao, "Simultaneous wireless power and information transmission based on harmonic characteristic of soft-switching inverter," *IEEE Trans. Ind. Electron.*, vol. 69, no. 6, pp. 6090–6100, Jun. 2022.

[12] L. Ji, L. Wang, C. Liao, and S. Li, "Simultaneous wireless power and bidirectional information transmission with a single-coil, dual-resonant structure," *IEEE Trans. Ind. Electron.*, vol. 66, no. 5, pp. 4013–4022, May 2019.

[13] Y. Fan, Y. Sun, X. Dai, Z. Zuo, and A. You, "Simultaneous wireless power transfer and full-duplex communication with a single coupling interface," *IEEE Trans. Power Electron.*, vol. 36, no. 6, pp. 6313–6322, Jun. 2021.

[14] G. Wei, J. Feng, J. Y. Zhang, C. Wang, C. Zhu, and S. Y. Ostanin, "An efficient power and data synchronous transfer method for WPT system using double-d coupling coil," *IEEE Trans. Ind. Electron.*, vol. 68, no. 11, pp. 10643–10653, Nov. 2021.

[15] Z. Yan, Z. Xiang, L. Wu, and B. Wang, "Study of wireless power and data transmission technology based on the triangular current waveform," *IEEE Trans. Power Electron.*, vol. 33, no. 2, pp. 1368–1377, Feb. 2018.